

# Analysis techniques for data from resonant-mass detectors

Pia Astone<sup>a</sup>

<sup>a</sup> INFN, at the Physics Dept. of “La Sapienza”, Rome (Italy)

## ABSTRACT

Resonant detectors of gravitational waves (g.w) have been operating for many years. These detectors allow to investigate various classes of signals, such as bursts, continuous waves, stochastic background. We will describe here some of the data analysis tools we have developed. In particular we will outline the problem of optimal filtering of the data, given the fact that the sensitivity of the detector is time varying, and some of the problems that arise when performing a coincidence analysis; we will describe some tools developed to look for signals from periodic sources, with a particular emphasis on the all-sky search we are running on the data of Explorer; we will describe the technique used to perform coincidences with Gamma Ray Bursts.

**Keywords:** gravitational waves, gravitational wave detectors, data analysis.

## 1. MAIN CHARACTERISTICS OF RESONANT DETECTORS

Resonant mass detectors of g.w. are cylindrical bars, whose end face vibrates when the bar is hit by a g.w.. The bar end face displacement  $\Delta L$  is proportional to the dimensionless wave amplitude  $h \approx \frac{\Delta L}{L}$ , where  $L$  is the length of the bar. The measurement of the displacement is done by means of transducers, well coupled to the bar, that convert the displacement into an electric signal. Resonant mass detectors have two resonance frequencies  $\approx (10 - 30)$  Hz apart, where the sensitivity is at its best. The parameters that determine the sensitivity are:

- the mass  $M$  of the bar. Given a material, the sensitivity improves with the mass;
- the bar temperature  $T$ . The sensitivity increases by cooling down the bar. In fact, the displacement of the bar due to the thermal noise depends on the square root of the temperature (the cooling of the bar brings also other advantages, such as the increasing of the merit factor and the possibility of using super-conducting, hence low-noise, devices);
- the merit factor  $Q$  of the bar-transducer system, proportional to the time the energy released by the signal remains into the bar. The higher the  $Q$  the better is the sensitivity.

Resonant bar g.w. detectors are<sup>1</sup>: **Allegro, Auriga, Explorer, Nautilus, Niobe**. After the joint effort of taking as much data as possible during the years 1997-2000, to perform the analysis with the **IGEC observatory**<sup>2</sup>, some apparatuses have been “switched off” to make important improvements<sup>3</sup>, and thus, at the time of this conference, only Explorer is in continuous operation and Allegro ran for 1 week in Jan 2002, in the new laboratory, showing that there was no damage caused by the move and that the new rotation system works. If we calculate the time coverage, that is the fraction of time over which at least one of the five detectors was working, from Jan, 1, 1997 up to May, 21, 2002, we get 1781/1966 days/days. This means, in case of an astronomical trigger, a coverage of 91%, over 5.4 years. The sensitivity to g.w. signals is determined by  $\tilde{h}$ , the **noise spectral amplitude** (or **strain sensitivity**), in units of  $1/\sqrt{\text{Hz}}$ . For example, for Nautilus 1999, at the resonances (and over a bandwidth of  $\simeq 1$  Hz):

$$\tilde{h} \propto \sqrt{T/(MQ)} = 3 \cdot 10^{-22} / \sqrt{\text{Hz}} \quad (1)$$

The bandwidth depends only on the transducer and amplifier. It can be increased by improving the coupling of the bar-transducer system and/or by reducing the noise temperature of the amplifier.

Resonant g.w. detectors allow to investigate various classes of signals:

---

Contact information: e-mail: pia.astone@roma1.infn.it; Web address: <http://www.roma1.infn.it/rog/astone>

**Table 1.** Main characteristics of Explorer and Nautilus, in the 2001 run

Parameters	Explorer	Nautilus
ON times	Mar-Dec	Jan-Dec
Bandwidth [Hz]	9	0.4
Bar T [K]	2.6	1.5
Duty cycle	267/294=91%	291/365=80%
Average sensitivity $h$	$4.5 \cdot 10^{-19}$	$5.7 \cdot 10^{-19}$
$M_0$ (in the GC)	$1.2 \cdot 10^{-4}$	$2 \cdot 10^{-4}$

- **Bursts**, that are signals from Supernova explosion, fall of a body into a black hole, final merge of the coalescence of a binary system. The expected signals are short pulses (a few ms each). The sensitivity to bursts  $h$  depends on  $\tilde{h}$  and on the bandwidth\*  $B$ . Optimum filters and coincidence analyzes are needed.
- **Continuous waves**, that are signals from rotating neutron stars or stars in binary systems. The signal is expected to be always present during the observation time. The sensitivity  $\tilde{h}$  to continuous waves depends on  $\tilde{h}$  and, at least ideally, on the square root of the observation time  $t_{obs}$ .
- **Stochastic background (SB)**, produced by a high number of uncorrelated events. At least two detectors, properly located and oriented, are needed. The sensitivity depends on the noise spectral amplitudes of both the detectors and on the square root of the overlapping frequency bandwidth and observation time.
- **Coincidences with gamma ray, neutrinos, (local) cosmic rays detectors**, data obtained with g.w. detectors can be analyzed in coincidence with data produced by astro-particle detectors.

In this paper, we will describe some of the data analysis tools developed for Explorer (at CERN) and Nautilus (at LNF), the detectors of the ROG (Rome, Frascati) collaboration. We will only give a general idea of various tools, and details can be found in the cited papers and in the references therein. Recent papers from the ROG collaboration can also be found at the address [www.roma1.infn.it/rog](http://www.roma1.infn.it/rog). In the year 2001, Explorer and Nautilus have worked with the best (average) ever reached sensitivity to bursts, and a very good duty cycle. Table 1 shows the major characteristics of the detectors during 2001. Nautilus has been turned off, at the beginning of 2002. The bar has been changed, and the new system will work at 935 Hz, where we expect a pulsar, as remnant of the SN1987A.

## 2. THE DETECTION OF BURSTS

The problem is the detection of very small signals, embedded in noise: the displacement produced by a signal emitted in a SN explosion that has released 1%  $M_0$  into g.w. in the Galaxy is  $h \approx 10^{-18}$ . This has to be compared with the displacement  $\Delta L$  produced by the noise, which depends on the square root of the bar temperature. For example,  $\Delta L = 10^{-17}$  m at the temperature  $T=3$  K,  $\Delta L = 3 \cdot 10^{-18}$  m at  $T=300$  mK. This is the core of the detection problem. To increase the  $SNR$ , defined as the ratio between the amplitude of a known shape signal  $h$  and the noise standard deviation  $\sigma_n$  it is necessary to filter the data, using **matched filters**. But the noise in the detectors is, in general, non-stationary and the design of the filter must face with this problem. **Adaptive filters** which use information on the actual noise are a good tool to solve this problem. We have compared the performances of (matched) adaptive and non-adaptive filters and results have been published<sup>4</sup>. More recently, we have done a detailed study and comparison of the performances of differently adapted filters. Some results are in<sup>5</sup>, and a work is in preparation<sup>6</sup>.

### 2.1. The adaptive implementation of the matched filter

The model of the noise of the system is the superposition of a white noise, due to the electronics, and a Brownian noise, that is the thermal noise of two mechanical oscillators at the resonance frequencies. In practice, even in good working

---

\*in the approximation of constant  $\tilde{h}$ , for  $SNR=1$  and for a 1 ms burst, we get:  $h = \frac{\tilde{h}}{0.001} \sqrt{\frac{2}{\pi B}}$ .

situations, spurious spectral peaks are present: adaptive filters react to the spurious lines by lowering the gain at the corresponding frequencies. This feature represents a good improvement in the sensitivity. However, it is not possible to find an unique optimum method of spectral estimation, since the goodness of the estimation depends on the behavior of the noise and various scenarios of are possible: presence of spurious, time varying, peaks in the spectra; presence of “short” time disturbances; presence of “long” time disturbances.

The *adaptive algorithms* are the methods used to estimate spectra from the data. The *criterion of selection* of the best filter is based on the experimental response of the filters.

It is shown in<sup>4</sup> that the SNR improvement introduced by a filter can be expressed in terms of a reduction of the temperature from the temperature  $T$  to the effective temperature  $T_{eff}$ :  $SNR_m/SNR_0 = T/T_{eff}$ , where  $SNR_0$  is the (energy) signal to noise ratio before the filtering and  $SNR_m$  is the (energy) signal to noise ratio after the filtering. For example, Explorer cooled at  $T = 2.7$  K has an effective temperature of  $T_{eff} = 1 - 5$  mK (this figure depends on the detector parameters and it increases with the bandwidth).  $T_{eff}$  [K] and  $h$ , the sensitivity to bursts, are related by:

$$h \simeq \frac{L}{\tau_g v_s^2} \sqrt{\frac{k T_{eff}}{M}} \quad (2)$$

where  $L$  is the bar length ( $L = 3$  m),  $M$  is the bar mass ( $M = 2300$  kg),  $v_s$  is the sound velocity in the bar ( $v_s = 5400$  m/s in Al),  $\tau_g$  is the pulse duration. Equation (2) holds if we suppose a constant noise spectrum over the detector bandwidth, that is a reasonable assumption. Numerically,  $h \simeq 7.97 \cdot 10^{-18} \sqrt{T_{eff}}$ , with  $T_{eff}$  in Kelvin and  $\tau_g = 1$  ms. Thus,  $T_{eff}=1$  mK means a sensitivity to bursts  $h \simeq 2.5 \cdot 10^{-19}$  ( $SNR = 1$ ). The best filter is, by definition, the filter that gives the best (lower) effective temperature, in case of rare events.

The procedure for estimating the spectra makes use of periodograms. The periodograms are exponentially and auto-regressively averaged with a given memory time. The recursive equation is:

$$S_i = P_i \cdot (1 - w) + S_{i-1} \cdot w \quad ; \quad w = \exp(-\Delta t/\tau) \quad (3)$$

where  $P_i$  is the last periodogram,  $S_i$  is the actual spectrum and  $w$  is the system memory by means of the time constant  $\tau$ .  $\Delta t = 105$  s is the time duration of each periodogram.

To face with possible scenarios of non-stationary noise, three different procedures for combining the periodograms have been implemented: the whole, clean and varying memory procedures and, consequently, the **whole, clean and varying memory matched filters**. All the procedures use Eq.(3), but they differ for the value of the time constant and for the criterion to accept the periodograms.

**The whole matched filter:** it is the simplest implementation of Eq.(3). In this case  $w$  is a constant and  $\tau = \tau_0$  is one hour. The algorithm uses all the periodograms to evaluate the filter. It is a good filter for stationary noise, quite a good filter for “long” disturbances, but it does not resolve the problem of the “short”, highly non stationary, disturbances (the estimation of the new periodogram is corrupted by the presence of the disturbance).

**The clean matched filter:** the problem of the “short” time disturbances, related to the abrupt presence of high excess noise, can be solved by eliminating the corresponding periodogram from the spectral estimation. “Short” means disturbances lasting for a time that is small compared to the time over which each periodogram is evaluated.  $w$  is constant, but the procedure uses only certain periodograms, to obtain a clean spectrum. The choice of the periodograms is done evaluating their integral  $s_P$  and comparing it with the expected value  $S_P$  (evaluated experimentally, using the past history of the data). Each periodogram is used to construct the clean filter only if  $s_P \leq k_s \cdot S_P$ , where  $k_s$  is chosen experimentally. Fig.(1) shows an example. A short but high disturbance has occurred at  $t \simeq 8$  hours. The behavior of the whole filter is degraded, even when the disturbance is over, while the clean filter recovers immediately the correct sensitivity.

**The varying memory matched filter:** when data are noisier, compared to the expectations, for a “long” time period, the results using the clean filter are no more as good as in the previous example. In fact the characteristics of the data are changed and the best spectral estimation is done using all the data. We have experienced that in case of noisy data, the behavior of the detector is much more non stationary. Thus, the procedure must “forget” the data more rapidly than usual, that is the memory time  $\tau$  adapts to the quality of the data. We call this filter **varying memory** or **adapted** filter. Following the observation that noisier data implies a less stationary system, we define  $\tau = \tau_0/(1 + \chi)$ , where  $\tau_0 = 1$  hour, and

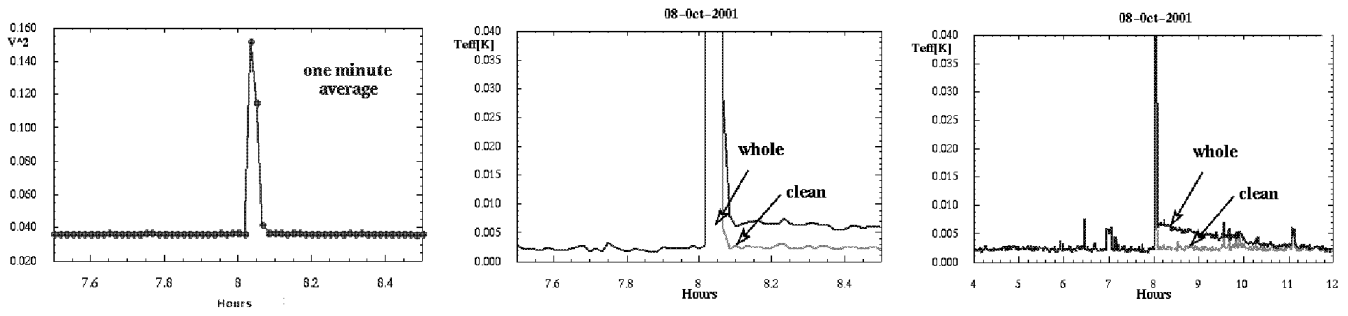


**Figure 1.** Highly non stationary noise. The left figure shows one minute averages of 1 hour of raw Nautilus data, in  $[V^2]$ , and middle and right figures show the  $T_{eff}$ , [K], obtained with the whole and clean matched filters, over 1 hour (middle) and over 9 hours (right), to show that it takes almost 2 hours to the whole filter to recover the true level of sensitivity (that is 2 mK), while the clean filter recovers immediately the correct sensitivity.

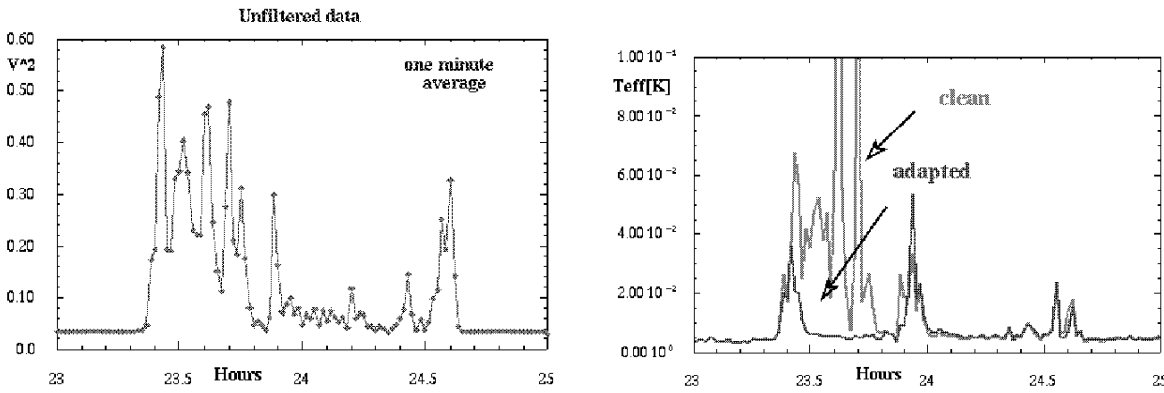


**Figure 2.** Comparison of the performances of the adapted and clean matched filters, in the case of  $\approx 40$  minutes excess noise. Left: one minutes averages of 2 hours of the raw  $[V^2]$  Nautilus data. Right: Comparison of the  $T_{eff}$  of the data filtered with the clean and adapted filters.

$\chi = s_P/S_P$ . The memory time  $\tau$  decreases during the noisy periods, as the ratio  $\chi$  increases. If  $\chi = 1$  (the actual noise of the periodogram equals the expectation),  $\tau = \tau_0$ . In case of good data,  $\chi \leq 1$ , and  $\tau$  increases toward the asymptotic value ( $2 \cdot \tau_0$ ). Fig.(2) shows (left) 1-minute averages of raw Nautilus data and (right) the  $T_{eff}$  obtained with the clean and adapted filters. During the excess noise, in the time period 23.3- 23.9 hours, the results are very different. The clean filter “follows” the raw data, and the noise temperature is higher than usual; the adapted filter is able to recover the problem, and the noise temperature is good, even during the disturbed period. In fact, we have verified that the higher noise is due to excess noise peaked around the minus mode, while the level of the white noise is constant. It takes only a few minutes to the filter to adapt to the new situation. A robust comparison of the filters implies to use also calibration signals, added to the noise of the detector at various level of  $SNRs$ . It is thus possible to evaluate the efficiency of detection of the filters, that is the ratio between the number of signals and the number of detected events, and the experimental parameters of the events, given the actual noise. We plan to add an on-line channel with simulated signals, in our acquisition system DAGA2-HF.

## 2.2. Coincidences between g.w. detectors

The search for bursts of gravitational radiation is based on the coincidence of detectors that have been operating simultaneously and have produced “event” lists. Various papers with results of coincidence analyzes done using cryogenic resonant detectors have been published<sup>7</sup>:

- 180 days of Explorer and Allegro data, from June until December 1991. No significant coincident excitations have been found and an upper limit on the rate of g.w. bursts has been put (less than 0.03 events/day at the level  $h > 2 \cdot 10^{-17}$ );
- 57 days of Explorer and Nautilus data, from February until November 1996, and 56 days of Explorer and Niobe data, from June until October 1995. No significant excess has been found, but various problems intrinsic to the coincidence analysis have been studied;
- 260 days of common observation with two or more detectors of the **IGEC** collaboration, from January 1997 until December 1998. No excess of coincidences has been found. The upper limit has been improved by a factor of three (less than 0.01 events/day at the level  $h > 2 \cdot 10^{-17}$ ); no g.w. bursts above  $h = 4 \cdot 10^{-18}$  have been detected.
- 94.5 days of Explorer and Nautilus data, from June until December 1998. The aim of this analysis, done on a subset of data exchanged within the IGEC collaboration, has been to study new algorithms.
- New data, that cover the period Jan 1997 - Dec 2000 have been exchanged. A new IGEC protocol has been followed, to exchange a more detailed information on the events. The new analysis has almost been completed<sup>8</sup> and a work is in preparation.

We are now analyzing Explorer and Nautilus 2001 data: we have 90 days of coincident operation at the level  $h \leq 6 \cdot 10^{-19}$  (hourly averages), selected from periods of data taking of a minimum length of 1 hour.

Relevant points of the coincidence analysis are listed here:

- when data are filtered, e.g. for delta-like **signals**, the output of the filter are **events**, above given thresholds. But, events are only an estimation of signals.
- the sensitivity of the detectors, and thus the threshold, varies with time;
- the sensitivities of the various detectors are, in general, different;

Thus, the same signal generates, in the detectors, events that give a different estimation and have a different uncertainty on the energy and on the time of arrival. For example, the Explorer and Nautilus sensitivity to bursts during the year 1998, was such that signals with amplitude  $h = 3 \cdot 10^{-18}$  could be seen, on the average, with good SNRs, using Nautilus and with much more poor SNRs, using Explorer. But, it is still worth to do the coincidence analysis (that cannot be done by thresholding the data and ignoring all the events obtained when the detector threshold was above the analysis threshold, which would correspond to the simplistic assumption that the efficiency of detection is 1, when the detector threshold is below the analysis threshold, and 0, when the detector threshold is above the analysis threshold). It is shown<sup>7</sup> that if the threshold was, in both the detectors, at  $SNR_t=20$  and if the signal had  $SNR_s=50$ , with Nautilus 1998, and  $SNR_s=20$ , with Explorer 1998, the *probability of detection* is 1 for Nautilus and 50% for Explorer<sup>†</sup>. We have thus proposed the use of algorithms based on the selection of the events on the basis of their compatibility with given signals.

---

<sup>†</sup> and, if the signal was lower, e.g.  $SNR_s=15$ , lower than the detector threshold, there is still a 30% probability of detecting it.

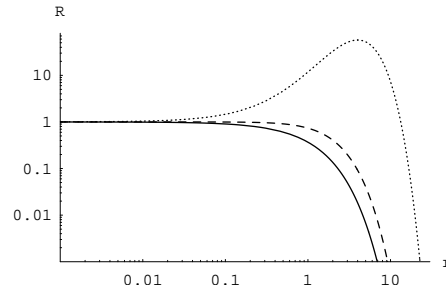


**Figure 3.** Relative belief updating ratio  $\mathcal{R}$  for the Poisson intensity parameter  $r$ , in units of events/month, inferred from an expected rate of background events  $r_b = 1$  event/month, and the following numbers of observed events: 0 (continuous); 1 (dashed); 5 (dotted).

### 2.3. On the procedure to put upper limits

A new algorithm to evaluate upper limits for a given source distribution on the sky has been proposed<sup>9</sup>. As shown, the algorithm used in the past does not fit with the following items:

- the energy of the measured event is not the energy of the signal;
- the efficiency of detection, for various thresholds and for the chosen source distribution on the sky, has to be taken into account.

In addition, the new procedure is based on a Bayesian approach, and some criticism on the usual way of reporting results in terms of “CL limits” is expressed. Our desiderata are well expressed by G. D’ Agostini in<sup>10</sup>: “the information contained in the experimental data should be presented in the most power and unbiased way”.

- The result should not depend on whether one believes that there is no effect, or that something has been found;
- the pieces of evidence coming from different experiments should be combined in the most efficient way;
- if many independent data sets each provide a little evidence in favor of the searched-for signal, the combination of all data should enhance the hypothesis;
- if the indications are incoherent, their combination should provide a stronger constraint against the hypothesis.

Probabilistic results depend necessarily on the choice of prior probability density function (p.d.f.), and in frontier research particular care has to be put, before stating probabilistic results. The Bayesian approach, thanks to the factorization between likelihood and prior, offers natural ways to present prior-independent results. The simplest idea would be just to provide the likelihood for each hypothesis under investigation. More conveniently, it has been proposed<sup>11</sup> to publish the likelihood rescaled to the asymptotic limit, where experimental sensitivity is lost. The reference value could be arbitrary, but for our problem we choose  $r_{REF} = 0$ , obtaining

$$\mathcal{R}(r; n_c, r_b) = \frac{f(n_c | r, r_b)}{f(n_c | r = 0, r_b)}, \quad (4)$$

where  $n_c$  is the number of measured coincidences;  $r$  is the g.w. rate, that is the quantity to be inferred;  $r_b$  is the measured background rate. The function  $\mathcal{R}$  has intuitive interpretations: it has the probabilistic interpretation of relative belief updating ratio, or the geometrical interpretation of shape distortion function of the p.d.f..  $\mathcal{R}$  goes to 1 for  $r \rightarrow 0$ , i.e. in the asymptotic region in which the experimental sensitivity is lost. As long as  $\mathcal{R} = 1$ , the shape of the p.d.f. (and therefore the relative probabilities in that region) remains unchanged. Instead, in the limit  $\mathcal{R} \rightarrow 0$  (for large  $r$ ) the final p.d.f. vanishes, i.e. the beliefs go to zero, no matter how strong they were before. Fig.(3) shows an example, the abscissa has been drawn in a log scale to make it clear that several orders of magnitude are involved. These curves transmit the result of the experiment immediately and intuitively:

- whatever one's beliefs on  $r$  were before the data, these curves show how one must<sup>‡</sup> change them;
- the beliefs one had for rates far above 20 events/month are killed by the experimental result;
- if one believed strongly that the rate had to be below 0.1 events/month, the data are irrelevant;
- the case in which no candidate events have been observed gives the strongest constraint on the rate  $r$ ;
- the case of five candidate events over an expected background of one produces a peak of  $\mathcal{R}$  which corroborates the beliefs around 4 events/month only if there were sizable prior beliefs in that region.

Moreover there are some technical advantages in reporting the  $\mathcal{R}$  function as a result of a search experiment:

- One deals with numerical values which can differ from unity only by a few orders of magnitude in the region of interest, while the values of the likelihood can be extremely low. For this reason, the comparison between different results given by the  $\mathcal{R}$  function can be perceived better than in terms of likelihood.
- Since  $\mathcal{R}$  differs from the likelihood only by a factor, it can be used directly in Bayes' theorem, which does not depend on constants, whenever probabilistic considerations are needed.
- The combination of different independent results on the same quantity  $r$  can be done straightforwardly by multiplying individual  $\mathcal{R}$  functions.

We can calculate the upper limit by solving the equation  $R(r, n_c, r_b) = 0.05$ . This limit is the *standard sensitivity bound*.

### 3. THE SEARCH FOR CONTINUOUS WAVES

The natural strategy for searching for monochromatic waves is to look for the significant peaks in the spectrum. In this case the SNR increases with the observation time  $t_{obs}$ : as  $t_{obs}$  increases, the frequency resolution of the spectrum increases - the frequency bin gets smaller  $\delta\nu = 1/t_{obs}$  - thus the noise content in each bin decreases with  $t_{obs}$ , while the signal is not dependent on the observation time. We use, to estimate the power spectrum, periodograms (squared modulus of the Fourier transform). For a periodic signal of amplitude  $\bar{h}$  at the frequency  $\bar{\nu}$  the periodogram gives  $\bar{h}^2$  with a noise contribution of  $2 S_h(\bar{\nu}) \delta\nu$ , being  $S_h(\bar{\nu})$  the two-sided noise power spectrum of the detector (measured in  $\text{Hz}^{-1}$ ). The SNR for periodic signals is:

$$SNR = \frac{\bar{h}^2 t_{obs}}{2S_h(\bar{\nu})} \quad (5)$$

Eq.(5) holds if the instantaneous frequency of the continuous signal at the detector is known. The analysis procedure in this case is "coherent", since the phase information is used. This is the case of "targeted searches", where the source parameters are all known (frequency, location, spin-down).

For a bar detector at the resonances the sensitivity is:

$$\bar{h} = 2.04 \cdot 10^{-25} \sqrt{\frac{T}{0.05 K} \frac{2300 kg}{M} \frac{10^7}{Q} \frac{900 Hz}{\bar{\nu}} \frac{1 day}{t_{obs}}}$$

where:  $T$  is the bar temperature,  $M$  its mass,  $Q$  the merit factor,  $\bar{\nu}$  the resonance frequency of the considered mode,  $t_{obs}$  the observation time, in days.

After **one year of effective observation**, the minimum detectable  $\bar{h}$  (SNR=1), using the parameters of the **Explorer** detector ( $T = 2 K$ ,  $M = 2300 kg$ ,  $Q = 10^6$ ), is  $\bar{h} = 2 \cdot 10^{-25}$  (and similar for **Allegro** and **Niobe**). For **Nautilus** and **Auriga**, if cooled at  $T = 100 mK$  and if  $Q = 10^7$ , the expected sensitivity at the resonances is:  $\bar{h} \simeq 1.5 \cdot 10^{-26}$ .

In most cases it is impossible to perform a coherent analysis over all the data: the procedure is limited by the needed computational power, which increases with high power of the observation time. This is the case of "blind searches",

---

<sup>‡</sup>It really is a 'must' and not a 'suggestion'. In fact, although probabilities may depend on individuals ('subjective'), the way they are updated follows from standard logic (yielding Bayes' theorem) and thus is 'objective'.

where the source parameters are unknown and an “all sky” search is needed. Hence, “hierarchical procedures” have been developed, which means that the observation time has to be divided in  $M$  sub-periods, such that the spectral resolution of the spectra becomes  $\delta\nu' = M/t_{obs}$  and the corresponding  $SNR$  is  $M$  times smaller than that in Eq.(5). These hierarchical strategies are based on iterations of two basic steps:

- coherent stage, where matched filtering on  $M$  chunks of data is done;
- incoherent stage, where the information from these chunks is combined, but the phase information is lost.

The  $M$  spectra can be combined together by incoherent summation, that is by averaging the square modulus (stacking procedure) or tracking lines in a time-frequency plane (tracking procedure, based on Hough transform, on which Potsdam and Rome groups are working). We remark that there are various ways to implement these procedures.

Fig.(4), left, shows an example of a time-frequency map obtained with Explorer 1991 data.

The Rome procedure is based on the construction of a Frequency Domain Data Base, data quality inspection, incoherent search with candidate selection (frequency, position, 2-3 spin-down parameters), coherent search on longer FFTs, only on the selected candidates, new incoherent and coherent steps on candidates, until the full length of data is reached. In the coherent step we partially correct the frequency shift due to the Doppler effect and spin-down, hence we can do longer FFTs and a better time-frequency map.

A collaboration between Rog-Virgo has been done, to apply to Explorer and Nautilus data the Rome strategy for the pulsar search. We have to develop the software for the “coherent steps”, including general tools. This software is the **PSS-astro library**, which is part of the libraries developed by the Virgo group in Rome. Documentation is available at the Web site (S. Frasca) <http://grwavsf.roma1.infn.it/pss>. Table 2 shows the index of the PSS-astro library. We are also developing the software for the creation of the Frequency Domain Data Base from our data, using tools in the **PSS** and **SNAG** libraries, done by S. Frasca. In this way, the analysis code is independent from the original data format. Our frequency domain data base consists of “elementary spectra”, each obtained by performing the FFT of a given number of samples. The sensitivity of each spectrum, according to Eq.(5), depends on its duration  $t_0$ . As our observations are affected by the Doppler shift, we have to choose the duration  $t_0$  the longest possible compatible with the requirement that the signal should “appear as monochromatic” during  $t_0$ . Clearly some assumptions about the frequency variation must be made. In principle, in order to achieve a higher SNR in the short spectrum, some preprocessing could take place by setting a coarse grid on the parameter space (i.e., the part of the sky that is being investigated) and performing suitable data stretching for each point in that parameter space. In this way a signal coming from that parameter space would appear as monochromatic in the resulting spectrum. As a consequence the size of the data base is increased by a factor equal to the number of points in parameter space, but there is a gain in SNR because of the higher spectral resolution. Up to now, to construct the Data Base, we have considered the whole sky and only the Doppler effect of the detector motion relative to the source, which has two periodic components. One is due to the revolution of the Earth over a period of 1 year and the second is due to the rotation of the Earth over a period of 1 sidereal day. They produce maximum time derivative of the frequency,  $b$  and  $a$ :

$$b = \left| \frac{d\nu_{orb}}{dt} \right|_{max} = \bar{\nu} 1.98 \cdot 10^{-11} \text{ Hz/s} ; \quad a = \left| \frac{d\nu_{rot}}{dt} \right|_{max} = \bar{\nu} 11.24 \cdot 10^{-11} \cos\phi \text{ Hz/s} \quad (6)$$

where  $\bar{\nu}$ , measured in Hz, is the intrinsic frequency of the source, and  $\phi$  is the latitude of the detector. The time duration  $t_0$  must be  $t_0 < \frac{1}{\sqrt{a+b}} = 8.7 \cdot 10^4 / \sqrt{\bar{\nu}}$  s, where we have put  $\cos\phi = 1$  (maximum possible value). In the case of Explorer 1991 we get  $t_0 < 10 \cdot 10^4 / \sqrt{\nu_0}$  s ( $\phi = 46$  deg). Thus, we have chosen  $t_0 = 2382.4$  s = 39.7 minutes<sup>§</sup>. Each elementary FFT has an header, containing information on the data, which can be used to set a threshold for vetoing the data. A preliminary coherent procedure has been applied to Explorer data, searching only for sources in the Galactic Center<sup>12</sup>: no signals with amplitude greater than  $h_c = 2.9 \cdot 10^{-24}$ , in the frequency range (921.32-921.38) Hz, were observed using data collected over a time period of 95.7 days, in 1991. An **overall sky search**, based on the procedure in<sup>13</sup> is now running on Explorer 1991 data. The data have been extracted from the Frequency Domain Data Base, following the procedure

<sup>§</sup> the maximum Doppler frequency variation (at 921.38 Hz) during  $t_0$  is 0.215 mHz, smaller than the frequency bin  $\delta\nu = 0.419$  mHz

**Table 2.** Index of the PSS-astro User Guide

Sections	Page
Introduction	2
JPL Planetary and lunar ephemerides	2
C-code to read the JPL files	3
Novas package (Novas.h, Novas.c)	4
Definition of the constants (Novascon.h Novascon.c)	10
The library PSS-astro (PSS-astro.h, PSS-astro.c)	11
Ephemeris file	11
Constant definitions	12
Astronomical time conversions	12
Modified from Novas.c	14
Functions used to read the jpl ephem file	15
Doppler effect	17
Einstein effect on the Doppler shift	17
Einstein effect on the Doppler shift (vector output)	17
Shapiro effect on the Doppler shift (vector output)	17
Detector velocity	18
Source position	18
Coordinate conversions	18
Vector utilities	19
elaboration of components	19
scalar product:	20
Appendix A: JPL ephemeris files and their use to get Doppler shift at the detector	21
Appendix B: Astronomical Times	23
Appendix C: Contributions to the Doppler effect	24
Appendix D: Tests with TEMPO	26

described in<sup>12,13</sup>. The analysis is carried out on the basis of a **Memorandum of understanding** between the **Rog** and the **Institute of Mathematics of the Polish Academy of Sciences**. We are analyzing two days of data over a bandwidth of 0.76 Hz, around 922 Hz. We have shown that we are able to perform an all-sky-2-days-long coherent search of the narrow-band data with no loss of signals of amplitude  $\bar{h} \geq 2.8 \cdot 10^{-23}$ . The 2-day stretch of data that we analyze in our all-sky search is taken from a larger continuous set of data of almost 13 days. UTC Time of the first sample of this set is 19th November 1991. Fig.(4), right, shows the strain sensitivity of the data. We have chosen an hexagonal grid over the sky and the number of filters we need to compute is  $N_{fft} \approx 3.7 \cdot 10^8$  (see<sup>13</sup>, Sect. VI and VII). The spin-down range is  $-9.17 \cdot 10^{-8} - + 9.17 \cdot 10^{-8}$  Hz/s. The search of the Northern sky is finished, and we have analyzed  $\approx 40\%$  of the Southern Sky. The analysis will be end by this year (2002). The highest SNR of a candidate is 7.9. Nevertheless all the “candidate signals” will be investigated thoroughly with accurate filters. We plan also to look for the candidates, using other days taken from the same run. Information on the progress and details of the analysis can be found at the Web site <http://www.astro.uni.torun.pl/kb/AllSky/AllSky.html>, written and maintained by Kazik Borkowski, where monthly bulletins, written by Andrzej Krolak, are published and sky maps updated monthly.

#### 4. COINCIDENCES WITH GAMMA RAY BURSTS

We have studied<sup>14</sup> Explorer and Nautilus 2001 data in correlation with the gamma ray burst data (GRB) obtained with the BeppoSAX satellite. The sensitivity of the detectors is not such to expect a physical results: in fact at the distances of the GRB sources ( $\approx 1$  Gpc), the g.w burst associated with a total conversion of 1-2 solar masses should have amplitude of the order of  $h \approx 3 \times 10^{-22}$ , while the present sensitivity for 1 ms g.w. pulses would require a total conversion of  $10^6$  solar masses at 1 Gpc. However, although detection of a gravitational signal associated with a single GRB appears hopeless, detection of a signal associated with the sum of many events could be more realistic. In the period 1 March through 17

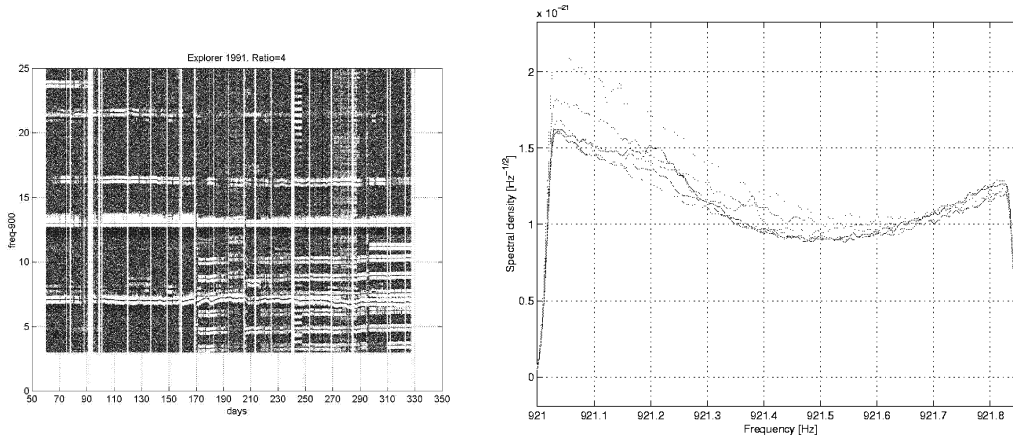


**Figure 4.** Left: Time-frequency map for the Explorer 1991 data. The calibration signal is at  $\approx 913$  Hz. Spurious lines can be noticed. Right: Plots of the strain sensitivity of consecutive 2-day stretches of data from the 13-day run. Note the stationarity of the data and their good sensitivity. Plots are on the linear and not on the usual log scale. Spectral density falls at the edges of the bandwidth because of the smoothing filter applied in the frequency domain.

July 2001 we have 101 BeppoSAX bursts, but only 47 occur at times when both antennas were operating. The statistical method we have used seems to us interesting, and we plan to use it on future data.

Searching for correlation between GRB and g.w. signals means dealing with the difference between the emission times for the two types of phenomena. Furthermore, the time difference can vary from burst to burst. We have used an algorithm based on cross-correlating the outputs of two g.w. detectors, thus coping with the problem of the unknown time difference between GRB and g.w. bursts. Hence it is essential to use at least two independent g.w. detectors: if simultaneous signals due to g.w. bursts arise both in the EXPLORER and NAUTILUS detectors, no matter when, with respect to the GRB arrival time, but within the chosen time window, we should find a larger value of the correlation function  $r(\tau)$  for  $\tau = 0$  s. Indicating with  $t_\gamma$  (trigger time) the initial time for the GRB's, for each burst we considered the g.w. data in  $t_m = 800$  s intervals centered at the  $t_\gamma$  ( $t_\gamma \pm 400$  s). The  $N_\gamma=47$  values of  $r(\tau)$ , one for each GRB, are used to calculate the average cross-correlation  $R(\tau)$ , shown in Fig.(5). No correlation at  $\tau = 0$  s is visible. Since we require the result in terms of g.w. amplitudes  $h$ , we need to relate cross-correlation quantities to energies. We have:

$$E_0 = T_{eff} \left( \frac{N_s}{N_\gamma} \right)^{1/4} \cdot \left( \frac{R_0}{\sigma_R} \right)^{1/2} \quad [\text{K}] \quad (7)$$

where  $N_s$  is the number of independent g.w. data,  $N_s \approx 7200$ ,  $\sigma_R$  is the standard deviation of our expectations of the dimensionless cross-correlation at zero delay time,  $R_0$ . The data are summarized by an observed average squared energy  $E_0^2 = -1.11 \times 10^{-3} \text{ K}^2$ , at  $-1.4$  standard deviations from the expected value in the case of noise alone.

According to the model, in the case of g.w. signals of energy  $E$ , we expect  $E_0^2$  to be a random number, modeled with a Gaussian probability density function around  $E^2$  with a standard deviation  $\sigma_{E^2}$ .  $E$  is the unknown quantity we wish to infer from the observed value of  $E_0$ : the probability inversion is obtained using Bayes' theorem (see<sup>11</sup> for a physics oriented introduction)

$$f(E_0^2 | E^2) \propto \exp \left[ -\frac{(E_0^2 - E^2)^2}{2\sigma_{E^2}^2} \right] ; f(E^2 | E_0^2) \propto f(E_0^2 | E^2) \cdot f_\circ(E^2) \quad (8)$$

where  $f_\circ(E^2)$  is the prior p.d.f. of observing g.w signals of squared energy  $E^2$ . We are eventually interested in inferring the g.w.'s amplitude  $h$ :

$$f(h | E_0^2) \propto f(E_0^2 | h) \cdot f_\circ(h) \quad (9)$$

where  $f(E_0^2 | h)$  is obtained by a transformation of  $f(E_0^2 | E^2)$ . As prior for  $h$  we considered a uniform distribution, bounded to non negative values of  $h$ , i.e.  $f_\circ(h)$  in Eq.(9) is a step function  $\theta(h)$ . This seems to us a reasonable choice and

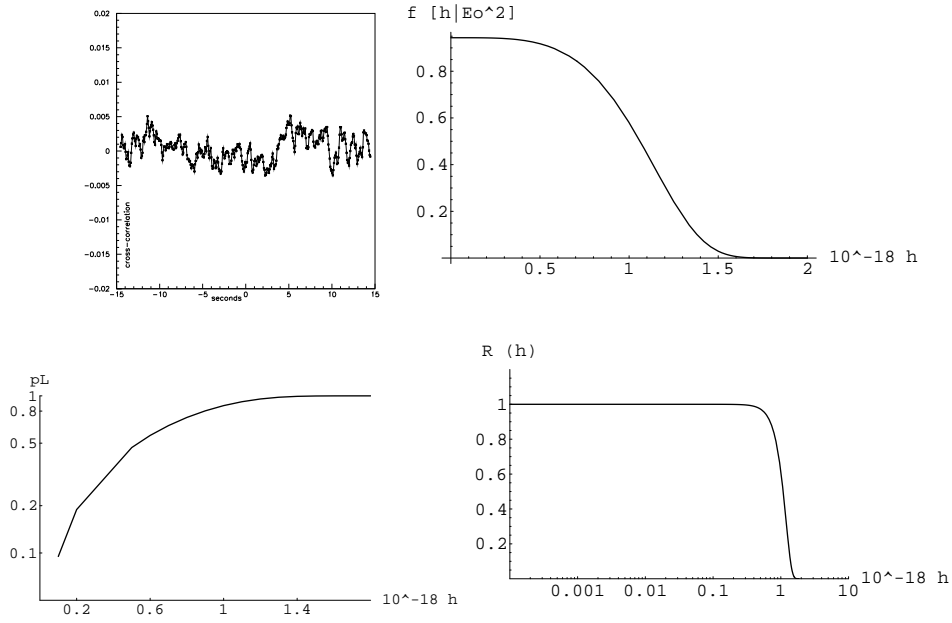


**Figure 5.** Left, top: cross-correlation  $R(\tau)$ , averaged over the 47 GRB's versus the time shift  $\tau$  in seconds. Right, top: p.d.f.  $f(h | E_0^2)$ . Left, bottom: upper limits  $p_L(h) \leq h$ . Right, bottom: relative belief updating ratio, as a function of  $h$ , plotted in log-linear scale.

it is stable, as long as other priors can be conceived which model the “positive attitude of reasonable scientists”<sup>¶</sup>. The probability density function of  $h$  is plotted in Fig.(5). The highest beliefs are for very small values, while values above  $1.5 \times 10^{-18}$  are practically ruled out. From the p.d.f.  $f(h | E_0^2)$ , in Fig.(5), we obtain an expected value and standard deviation for  $h$  of  $0.56 \times 10^{-18}$  and  $0.35 \times 10^{-18}$ , respectively, which fully account for what is perceived as a null result. We have excluded the presence of signals of amplitude  $h \geq 1.2 \times 10^{-18}$ , with 95 % probability, if we allow a time delay between g.w. bursts and GRB within  $\pm 400$  s, and  $h \geq 6.5 \times 10^{-19}$ , if the time delay is within  $\pm 5$  s.

Probabilistic results depend necessarily on the choice of prior probability density function of  $h$ . For example, those firmly convinced that g.w. burst intensities should be in the  $10^{-22}$  region would never allow a 5% chance to  $h$  above  $1.2 \cdot 10^{-18}$ . The likelihood for each hypothesis under investigation, is, in this case,  $f(E_0^2 | h)$  and the relative belief updating ratio (see Fig.(5), where the choice of the log scale for  $h$  is to remember that there are infinite orders of magnitudes where the value could be located. ) is:

$$\mathcal{R}(h) = \frac{f(E_0^2 | h)}{f(E_0^2 | h_{ref} = 0)} \quad (10)$$

This function gives the Bayes factor of all  $h$  hypotheses with respect to  $h = 0$ : up to a fraction of  $10^{-18}$  the experimental evidence does not produce any change in our belief, while values much larger than  $10^{-18}$  are ruled out. The region of transition from  $\mathcal{R}$  from 1 to zero identifies a *sensitivity bound* for the experiment. The exact value of this bound is a matter of convention, and could be, for example, at  $\mathcal{R} = 0.5$ , or  $\mathcal{R} = 0.05$ . We have  $1.3 \times 10^{-18}$  and  $1.5 \times 10^{-18}$ , respectively.

<sup>¶</sup>A prior distribution alternative to the uniform can be based on the observation that what often seems uniform is not the probability per unit of  $h$ , but rather the probability per decade of  $h$ , i.e. researchers may feel equally uncertain about the orders of magnitudes of  $h$ . This prior is known as Jeffreys' prior, but, in our case, it produces a divergence for  $h \rightarrow 0$  in Eq.(9), a direct consequence of the infinite orders of magnitudes which are equally believed. To get a finite result we need to put a cut-off at a given value of  $h$

## 5. THE SEARCH FOR STOCHASTIC BACKGROUND

We want now briefly recall that a limit,  $\Omega_{gw} \leq 60$ , has been put by cross-correlating few hours of Explorer and Nautilus data in the year 1997<sup>3</sup>. The analysis procedure is based on the evaluation of cross-spectra, which can be easily done using the Frequency Domain Data Base. Limits on  $\Omega_{gw}$  less than the unity can be achieved cross-correlating data from a bar/bar couple or from a bar/interferometer couple. For example, the cross-correlation of 4 months of Nautilus and Auriga data, at the sensitivity expected in the next 2003 run, would put the limit  $\Omega_{gw} \leq 0.1$ ; joint analyzes with Virgo, Nautilus and Auriga may put limits at the level  $\Omega_{gw} \leq 3 - 5 \cdot 10^{-3}$  (with 1 year of integration, the expectations for Nautilus and Auriga (Phase II), and  $\tilde{h}(@900 Hz) \simeq 10^{-22} / \sqrt{Hz}$  for Virgo). The two groups Ligo and Allegro, operating two detectors 40 km apart, have planned to do SB searches, as soon as both the detectors will be operative.

## 6. CONCLUSIONS

We have presented a general idea of some analysis tools we have developed to analyze data from resonant detectors. We have referenced only a few papers, I invite you to refer also to references therein. Basically, the detection problem is related to the low SNRs, to the non-stationary noise of detectors, and to the high computing power. Detection of g.w.'s is a very important task in frontier research physics and collaboration with the entire g.w. community is essential to reach the goal, for which we are all so hardy working.

## REFERENCES

1. Allegro: <http://gravity.phys.lsu.edu>; Auriga: <http://www.auriga.lnl.infn.it>; Explorer, Nautilus: <http://www.roma1.infn.it/rog>; Niobe: <http://www.gravity.pd.uwa.edu.au>
2. IGEC site on the WEB: <http://igec.lnl.infn.it/>
3. P. Astone, "Resonant mass detectors: present status" *CQG* **19**, pp. 1227-1535 (2002)
4. P. Astone, C. Buttiglione, S. Frasca, G.V. Pallottino, G. Pizzella, "The fast matched filter for g.w. data analysis", *Nuovo Cimento*, **20C**, pp.9-60, (1997)
5. S. D'Antonio, "The online data filters for Explorer and Nautilus" *CQG* **19**, pp. 1499-1505 (2002)
6. P. Astone, S. D' Antonio, S. Frasca, M. A. Papa, in preparation (July 2002)
7. P. Astone, S. D' Antonio, G. Pizzella, "Coincidence analysis in g.w. experiments", *CQG* **19**, pp. 1443-1448 (2002)
8. P. Astone et al, "Search for g.w. bursts by the network of resonant detectors", *CQG* **19**, pp. 1367-1370 (2002)
9. P. Astone, G. Pizzella, "On upper limits for g.w. radiation" *Astroparticle Physics* **16**, pp. 441-450 (2002)
10. G. D'Agostini, " Minimum Bias Legacy of Search Results" *Nuclear Physic B (Proc. Suppl.)* **109B** pp. 148-152 (2002)
11. G. D' Agostini *Bayesian reasoning in high-energy physics: principles and applications* CERN 99-03 (1999) This report and related references can be found at the URL: <http://www-zeus.roma1.infn.it/agostini/prob+stat.html>
12. P. Astone et al., "Search for periodic g.w. sources with the Explorer detector" *PRD* **65**, 022001 (2002) (gr-qc/0011072)
13. P. Astone, P. Borkowsky, P. Jaranowsky, A. Krolak, "Data analysis of g.w. signals from spinning neutron stars. IV: an all-sky search" *PRD* **65**, 042003 (2002) (gr-qc/0012108)
14. P. Astone et al., "Search for correlation between GRB's detected by BeppoSax and g.w. detectors Explorer and Nautilus" submitted to *PRD* (Jul 2002) (astro-ph/0206431).